APH N.S., Heavy Ion Physics **xx** (2001) xxx–xxx

HEAVY ION PHYSICS
©Akadémiai Kiadó

Nucleon Coalescence in the Interaction of ^{16}O with ^{59}Co at an Incident Energy of 250 MeV

E.Gadioli[1], G.F.Steyn[2], C.Birattari[1], C.Catarisano[1], M.Cavinato[1], S.H.Connell[3], E.Fabrici[1], S.V.Förtsch[2], E.Gadioli Erba[1], J.J.Lawrie[2], F.M.Nortier[2], J.P.F.Sellschop[3], E.Sideras Haddad[3]

[1] Dipartimento di Fisica, Universita′ di Milano,
Istituto Nazionale di Fisica Nucleare,
via Celoria 16, 20133 Milano, Italia
[2] National Accelerator Centre,
PO Box 72, Faure 7131, South Africa
[3] University of the Witwatersrand, Johannesburg,
Schonland Research Centre for Nuclear Sciences, PO Wits 2050, South Africa

Received 8 October 2001

Abstract. We have observed the emission of intermediate mass fragments with a maximum yield at the Coulomb barrier energy in the interaction of 250 MeV ^{16}O ions with ^{59}Co. These emissions, which become dominant at emission angles larger than 20°, are explained by assuming that they are produced by nucleon coalescence during the thermalization of the composite nuclei produced in the complete and incomplete fusion of ^{16}O with ^{59}Co.

Keywords: Nucleon coalescence; Fragment production
PACS: 25.70.Gh Compound nucleus - 25.70.Mn Projectile and target fragmentation

1. Introduction

In reactions induced by light nuclei one observes quite a copious production of projectile-like fragments. One mechanism responsible for such emissions is the binary fragmentation (or break-up) of the projectile. Fragments produced by this mechanism are observed at forward angles and display a broad peak at about the beam velocity. At rather small projectile energies, below about 10 MeV/amu, the spectra of these fragments are symmetric and have approximately gaussian shapes. These features do not change with increasing emission angle [1]. This scenario changes notably with increasing projectile energy. It was found some time ago [1-4]

1219-7580/99/ \$ 5.00

that, at energies above about 15 MeV/amu, pure "break-up" spectra are observed only at the most forward angles and are asymmetric, showing quite a steep fall-off on the high energy side and a longer tail extending up to the Coulomb barrier on the low energy side. This behaviour is confirmed by the data discussed in this paper concerning the interaction of ^{16}O with ^{59}Co at an incident energy of 250 MeV. At larger emission angles ($\theta \geq 20°$) the characteristic shape corresponding to a pure break-up mechanism disappears. The average energy of the emitted fragments decreases quite rapidly with increasing θ and, for $\theta \geq 30°$, the spectra are dominated by quite a sharp peak at about the Coulomb barrier energy.

This low energy component in the spectra of intermediate mass fragments (IMFs) was attributed by Hussein *et al.* [4] to some complex pre-compound process which is unrelated to the break-up of the projectile. However, to our knowledge, a quantitative description of this contribution was not proposed.

In this paper we deal with the theoretical interpretation of this contribution to the measured spectra. It is suggested that it may be satisfactorily reproduced by assuming that it is due to the coalescence of nucleons into the observed fragments during the thermalization of the composite nuclei produced in the complete fusion of the projectile with the target nucleus, or in the fusion of a fragment produced in the projectile's break-up.

In Section **2** a brief sketch of the experimental set-up is given. Section **3** is devoted to a discussion of the theoretical approach and Section **4** to the comparison of the theoretical expectations with the data, followed by the conclusions.

2. Experimental Procedure

The experiment was performed at the cyclotron facility of the National Accelerator Centre in Faure, South Africa. A 250 MeV ^{16}O beam was focused to a spot of about 3 mm in diameter on a 1 mg/cm^2 thick ^{59}Co target during several days of data acquisition. Inclusive spectra of several projectile's fragments were measured using two identical detector telescopes mounted in a 1.5 m diameter scattering chamber. Each telescope consisted of a 25 μm thick Si surface barrier ΔE detector, followed by a 2 mm thick Si surface barrier stopping (E) detector. The standard ΔE-E technique was used for particle identification. Passive brass collimators were used to define solid angles of 0.7 msr.

Energy calibration of the Si detectors were performed using both the kinematics of elastic scattering and α particles from a ^{228}Th source. Beam halo was monitored frequently by comparing the count rate from an empty target frame with that of the rate from the ^{59}Co target. Standard electronics together with an on-line computer were used to write event-by-event data to magnetic tape for subsequent off-line analysis. Electronics dead time never exceeded 5% at the most forward angles and were generally well below 1% at angles larger than 10°.

Data were collected at several scattering angles between 4° and 50°. The cross sections are believed to be accurate to within a systematic error of 10%.

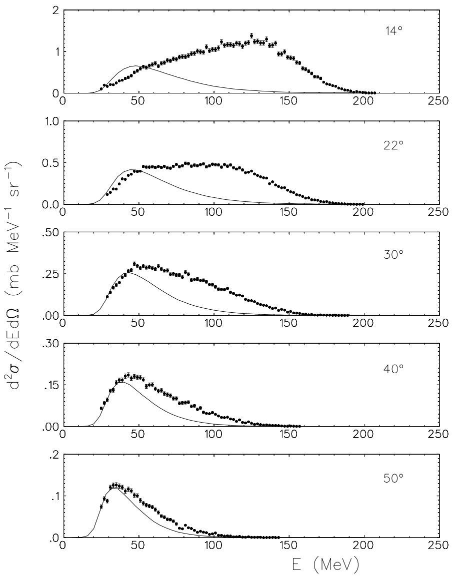

Fig. 1. Spectra of B fragments emitted in the interaction of 250 MeV ^{16}O ions with ^{59}Co. The experimental data are given by the black points and the coalescence contributions by the full lines.

The measured IMF spectra are shown at a few selected angles in Figs. 1 to 3. These figures show that at the most forward angles the spectra are dominated by the break-up contribution which, however, decreases rapidly with increasing emission angle. In contrast, even if the clusters produced by coalescence are preferentially emitted at forward angles, the predicted *coalescence* contribution, calculated as discussed below, is negligible with respect to break-up at the most forward angles but becomes dominant at larger angles. The break-up contribution is not discussed in detail in this paper since the focus is primarily on the role of the coalescence contribution. However, in order to point out that the break-up mechanism is quite well understood, we include in Fig. 2, for the case of the emitted carbon ions, the predictions of this component, calculated as proposed in [1].

3. Theoretical Calculations

The coalescence model [5,6] was first proposed, in heavy-ion reactions, to account for the spectra of the light composite ejectiles. Subsequently it was notably improved by some of the present authors and also used to predict the emission of IMFs [7,8]. The model is based on the assumption that, during the intranuclear interaction cascade through which the initial orderly kinetic energy of the two fusing ions transforms into random thermal energy, an IMF may be produced by coalescence of nucleons

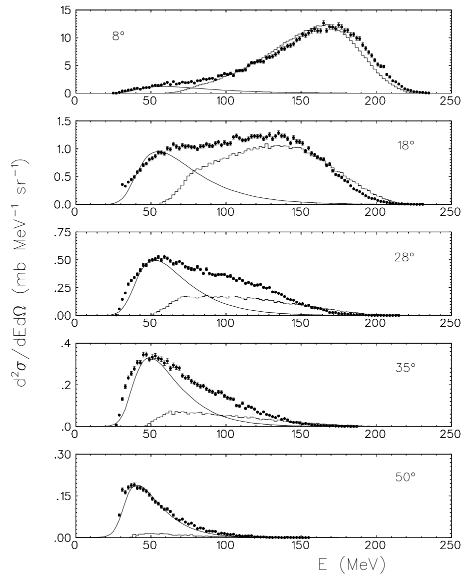

Fig. 2. Spectra of C fragments emitted in the interaction of 250 MeV ^{16}O ions with ^{59}Co. The experimental data are given by the black points, the coalescence and the break-up contributions by the full lines and the histograms.

whose momenta fall into a sphere of radius $p_{c,F}$ in momentum space. This happens with the largest probability when the directions of the excited nucleons still show a high degree of correlation, as is expected in the initial stages of the intranuclear interaction cascade.

In our approach the evolution of the excited system towards equilibrium is simulated by a set of Boltzmann Master Equations (BME) the solution of which, in the assumption of azimuthal symmetry, gives the occupation probability $n(\epsilon, \theta, t)$ of the nucleon states as a function of the energy ϵ, the angle θ between the nucleon and the projectile direction, and the time t [9,10]. To evaluate $n(\epsilon, \theta, t)$ we define a set of bins which, apart from boundary effects, have a constant volume in the momentum space. As long as one considers mean values one may assume azimuthal symmetry with respect to the beam direction, thus one can use only two independent variables, p^2 and p_z, the component of the linear momentum along the beam axis. The bins are thus characterized by constant values of Δp^2 and Δp_z. The bin indexes i, j, l, m in the following set of BME characterize momentum space intervals with volume $V_p \propto \Delta\epsilon\Delta p_z$ centered around given values of the energy ϵ_i, and $(p_z)_i$. Moreover, considering elastic intranuclear interactions, the internal transitions bring the nucleons from the centre of one bin to the centre of another one. With an appropriate ordering of the bins one may label each bin by only one index and, describing the nucleus as a two-fermion gas, one may write formally the set of BME

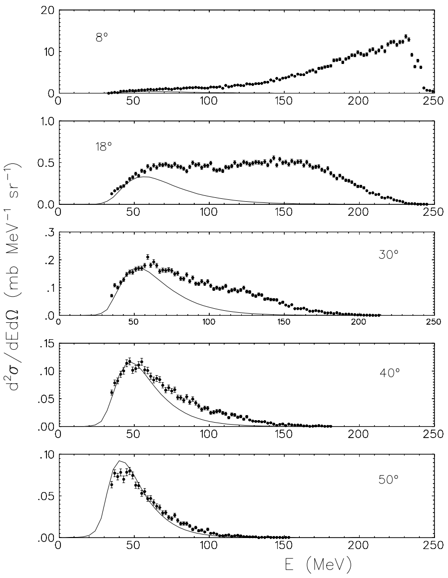

Fig. 3. Spectra of N fragments emitted in the interaction of 250 MeV ^{16}O ions with ^{59}Co. The experimental data are given by the black points and the coalescence contributions by the full lines.

for the proton and the neutron gases. That for the proton gas is

$$\frac{d(n_i g_i)^\pi}{dt} = \sum_{jlm}[\omega^{\pi\pi}_{lm\to ij} g^\pi_l n^\pi_l g^\pi_m n^\pi_m (1-n^\pi_i)(1-n^\pi_j)$$

$$-\omega^{\pi\pi}_{ij\to lm} g^\pi_i n^\pi_i g^\pi_j n^\pi_j (1-n^\pi_l)(1-n^\pi_m)] + \sum_{jlm}[\omega^{\pi\nu}_{lm\to ij} g^\pi_l n^\pi_l g^\nu_m n^\nu_m (1-n^\pi_i)(1-n^\nu_j)$$

$$-\omega^{\pi\nu}_{ij\to lm} g^\pi_i n^\pi_i g^\nu_j n^\nu_j (1-n^\pi_l)(1-n^\nu_m)] - n^\pi_i g^\pi_i \omega^\pi_{i\to i'} g^\pi_{i'} \delta(\epsilon^\pi_i - \epsilon^\pi_F - B^\pi_i - \epsilon^\pi_{i'}) - \frac{dD^\pi_i}{dt}, \quad (1)$$

where π and ν indicate, respectively, the protons and the neutrons. An analogous set of equations holds for the neutron gas.

The quantities g_i are the total number of states in bin i. The quantities $\omega_{ij\to lm}$, $\omega_{i\to i'}$ and dD_i/dt are, respectively, the internal transition decay rates, the decay rates for emission of single protons of the i-th bin into the continuum, and a depletion term which accounts for the emission of protons of the ith bin which are part of a cluster. The expressions of these terms are given in [7-10] and do not need to be repeated here.

The multiplicity spectrum of the nucleons emitted with energy $\epsilon' = \epsilon - \epsilon_F - B$

(B and ϵ_F are the nucleon binding and Fermi energies) is given by

$$\frac{d^2M_n(\epsilon',\theta)}{d\epsilon' d\Omega} = \frac{1}{2\pi \sin\theta} \int n(\epsilon,\theta,t) \frac{\sigma_{inv,n} v_n}{V} \rho_n(\epsilon',\theta) dt, \qquad (2a)$$

where $\sigma_{inv,n}$ is the inverse process cross section, v_n the relative velocity between the emitted nucleon and the residual nucleus, and V the laboratory volume which cancels with an equal term which appears in the expression of the density of particle states in the continuum $\rho_n(\epsilon',\theta)$. A similar expression is used for evaluating the multiplicity of the emitted composite particles and IMFs (hereafter referred to as *clusters*):

$$\frac{d^2M_c(E'_c,\theta_c)}{dE'_c d\Omega} = \frac{R_c}{2\pi \sin\theta} \int N_c(E_c,\theta_c,t) \frac{\sigma_{inv,c} v_c}{V} \rho_c(E'_c,\theta_c) dt, \qquad (2b)$$

where R_c is a numerical factor (≤ 1) which gives the survival probability of the cluster (i.e. the probability of escaping before dissolving again into its constituents). The cluster state occupation probability $N_c(E,\theta_c,t)$ is a function of the state occupation probabilities $n(\epsilon,\theta,t)$ of the nucleons constituting the cluster and is given, for a cluster made by Z_c protons and N_c neutrons, by :

$$N_c(E,\theta_c,t) = \Pi_i (n_i^\pi(\epsilon,\theta,t))^{P_i(E_c,\theta_c)Z_c} \cdot \Pi_i (n_i^\nu(\epsilon,\theta,t))^{P_i(E_c,\theta_c)N_c}, \qquad (3)$$

where the index i runs over all the bins in which the states of the protons and the neutrons constituting the cluster may be found and $P_i(E_c,\theta_c)$ is the fraction of bin i which falls within the Fermi sphere of the cluster c [8].

In our previous calculations of the IMF spectra we could not evaluate with the BME the angular dependence of the nucleon state occupation numbers $n(\epsilon,\theta,t)$, and, since the correlation probability of nucleons critically depends on the anisotropy of their momentum distribution, we were forced to use quite arbitrarily the initial momentum distribution in the first steps of the intranuclear cascade and, abruptly, an isotropic one after a given number of steps. This assumption permitted to reproduce reasonably well the hardest part of the light cluster's angle integrated spectra. The improved version of the BME which we use now [9,10] giving the angular dependence of the nucleon state occupation probabilities $n(\epsilon,\theta,t)$ allows one to evaluate the cluster's angular distributions without introducing arbitrary assumptions.

Clusters of a given type may be produced not only in the complete fusion (CF) of the projectile and the target but also in an incomplete fusion (ICF), when only part of the projectile fuses with the target nucleus.

$$\frac{d^2\sigma}{dE'_c d\Omega} = \sigma_{cf} \frac{d^2M_c^{CF}(E'_c,\theta_c)}{dE'_c d\Omega} + \sum_i \sigma_{ICF,i} \frac{d^2M_c^{ICF,i}(E'_c,\theta_c)}{dE'_c d\Omega}. \qquad (4)$$

Likely, the most important of the incomplete fusion reactions is the incomplete fusion of a ^{12}C fragment. Incomplete fusion of ^{8}Be is presumably small since fragmentation of ^{16}O into ^{8}Be fragments is hindered by the quite large fragmentation energy. Even less likely is the fragmentation of ^{16}O into B and Li, as is shown by the low cross section for B production by ^{16}O break-up which we have measured in this experiment.

However the cross section for incomplete fusion of ^{12}C, σ_C, may be quite large (up to about 500 mb) as is discussed in the Appendix. Fig. 4 shows that in this

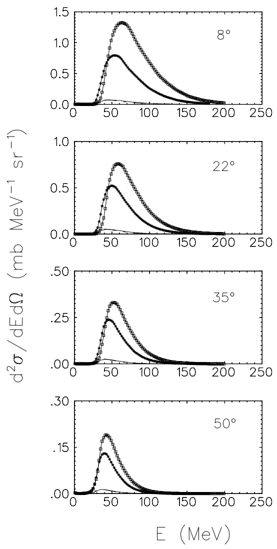

Fig. 4. Contributions of complete and incomplete fusion reactions to the calculated coalescence spectra for C. The highest in absolute value is that of complete fusion. The second in magnitude is due to the incomplete fusions of a ^{12}C. The lowest are those due to ^{10}B and ^{8}Be incomplete fusion which are almost indistinguishable and are superimposed. In these calculation R$_c$ was taken equal to 1.

case the contribution of the incomplete fusion of a ^{12}C to the coalescence spectra might be about 60% of that due to the ^{16}O complete fusion.

The continuum energy of the cluster c, E'_c is given by

$$E'_c = E_c - S_c - A_c(E_{CN,F} - E_{c,F}), \tag{5}$$

as suggested in [8], where S_c is the cluster separation energy and $E_{CN,F}$ and $E_{c,F}$ are the composite nucleus and the cluster Fermi energies.

We used the values given in our previous BME calculations [7-11] for most of the input parameters necessary for evaluating $d^2\sigma/dE'd\Omega$. Here we discuss only those parameters which affect the calculated cross sections more significantly. The first is the emitted cluster Fermi energy $E_{c,F} = p^2_{c,F}/2m$ (m is the nucleon mass). Even if this might be used as a free parameter, varying its values within a reasonable range of values, in order to improve the agreement between the calculated and the experimental spectra, we used for it values chosen *a priori* given by:

$$E_{c,F} = \frac{1}{A}[ZE^{\pi}_{c,F} + NE^{\nu}_{c,F}], \tag{6}$$

where $E^{\pi}_{c,F}$ and $E^{\nu}_{c,F}$ are, respectively, the Fermi energy of the cluster's protons and neutrons. As suggested in [11], these are given by

$$E^{\pi}_{c,F} = E_F(\frac{2Z}{A})^{2/3}(1-0.387A^{-1/3})^2, \tag{7a}$$

and

$$E^{\nu}_{c,F} = E_F(\frac{2N}{A})^{2/3}(1-0.387A^{-1/3})^2, \tag{7b}$$

where Z, N and A are the proton, neutron and mass numbers and E_F is the nuclear matter Fermi energy for which we adopted the value of 43.5 MeV. Fig. 5 shows

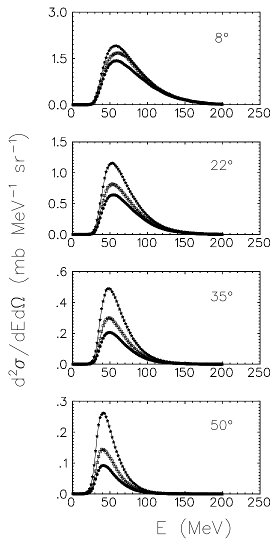

Fig. 5. Spectra of C produced by coalescence in the ^{16}O complete fusion for different values of the cluster Fermi energy. The highest in value is for E_F=43.5 MeV, the second in magnitude for E_F=41.4 MeV and the smallest for E_F=40 MeV. In these calculation R_c was taken equal to 1.

the sensitivity of the calculation to $E_{c,F}$. Here the contribution of complete fusion to the calculated spectra is given for E_F values of 43.5. 41.4 and 40 MeV. With increasing E_F, the coalescence cross section increases in absolute value and shows a weaker angular dependence. The first effect is obvious, the second is due to the fact that with increasing the cluster Fermi energy its constituent nucleons may have more diverging directions.

Another important calculation parameter is the effective Coulomb barrier which the clusters feel at the moment of emission. The experimental spectra show that the clusters may be emitted with rather low energy indicating a low effective Coulomb barrier V_c. In addition, the assumption that the clusters are emitted by recoiling spherical nuclei (V_c = const), leads to a quite sensible angular dependence of the calculated barriers in the Lab. system. These are too high for the particles emitted in the forward direction and too low for those emitted at larger angles, in disagreement with the experimental results. This difficulty may be overcome if, when the cluster is emitted, the nucleus is deformed and stretched in the forward direction. In this case the barrier increases with emission angle in the recoiling nucleus frame. Assuming that the emitting nucleus is a rotation ellipsoid with a ratio of the minor to the major axis $b/a \approx 0.6 - 0.7$, one may reasonably reproduce at all the angles the observed spectral shapes at the lowest emission energies. As in our previous calculations we used, for simplicity, semiclassical expressions for the emitted cluster inverse cross sections

$$\sigma_{inv,c} = \sigma_{geo}(\theta)(1 - \frac{V_c(\theta)}{E_{ch}}), \tag{8}$$

where E_{ch} is the channel energy and $\sigma_{geo}(\theta)$ and $V_c(\theta)$ are the geometrical cross section and the Coulomb barrier in the recoiling nucleus reference frame which depend now on the cluster's emission angle. To avoid the sharp and not realistic low energy edge of these semiclassical expressions and to take into account the possibility of cluster emission below the barrier, we used for $\sigma_{inv,c}$ at emission energies slightly below and around the Coulomb barrier an expression evaluated with the Hill and Wheeler parabolic approximation [12].

The absolute value of $d^2\sigma/dE'd\Omega$ also depends on the number of the clusters of a given type which are emitted and their excitation energy. In our experiment the different isotopes of a given fragment are not separated, as also happens in many experiments discussed in the literature. We thus assumed that several isotopes may contribute to the coalescence spectra for each observed fragment: ^{8}B to ^{14}B for B, ^{9}C to ^{16}C for C and ^{12}N to ^{17}N for N. The clusters may also be produced in excited states [13] which decay to the cluster's ground state before detection. The rather high value we use for E_F may be an effective way to include these emissions. The clusters might also be produced in states which decay by particle emission and thus contribute to the yield of the lighter fragment. This contribution should however be small because the coalescence probability decreases rapidly with increasing cluster mass.

4. Comparison with the Experimental Data and Conclusions

In Figs. 1 to 3 the spectra of B, C and N emitted at a few selected angles are compared with the calculated coalescence spectra. In the case of C the estimated break-up contribution is also shown. The calculations reproduce very satisfactorily the data with the only exception being the B spectra at emission angles below about 20°. As discussed in the previous Section most of the calculation parameters were fixed *a priori* and were not subsequently varied to improve the agreement with the data. The values of R_c which are required to reproduce the observed absolute values were found to be $\approx$ 0.13, 0.55 and 0.26 for, respectively, B, C and N. These values should not be taken to literally due to the complexity of the calculation, the approximations made and the *a priori* choice of most of the calculation parameters, especially the Fermi energies of the clusters. These, in the case of light fragments, could appreciably differ from the values calculated with (7a,b) which must be considered more realistic for higher mass fragments. What matters more is the fact that these calculations give the correct order of magnitude and do not underestimate significantly the yield of the low energy IMF which we measure.

To conclude, we may be rather confident that our approach reproduces quite correctly the emission of the observed low energy IMFs in the hypothesis that they are produced by nucleon coalescence during the thermalization of the composite nuclei created in the fusion of the projectile and the target or of projectile fragments with the target. It is also noteworthy that our model predicts a negligible emission of coalescence IMFs at an incident ^{16}O energy of 100 MeV, in agreement with subsequent measurements we performed which show that all the IMFs observed at this energy are produced by projectile break-up. We also have to stress that the calculations which we discuss in this paper reproduce accurately the spectra of nucleons and light clusters which are emitted during the thermalization of the excited nuclei produced in the interaction of two ions [7,9,10].

Appendix

In our present calculations we assumed that four terms mainly contribute to the coalescence spectra: the complete fusion of ^{16}O, and the incomplete fusion of ^{12}C, ^{10}B and ^{8}Be fragments produced in the ^{16}O break-up. Incomplete fusion of lighter fragments was not considered because, in the coalescence model, they give a small contribution to the production of fragments of substantially higher mass.

The theoretical *coalescence* spectra are thus assumed to be given by

$$\frac{d^2\sigma}{dE_c' d\Omega} = \sigma_{cf} \frac{d^2 M_c^O(E_c',\theta_c)}{dE_c' d\Omega} + \sigma_C \frac{d^2 M_c^C(E_c',\theta_c)}{dE_c' d\Omega} + \sigma_B \frac{d^2 M_c^B(E_c',\theta_c)}{dE_c' d\Omega}, \sigma_{Be} \frac{d^2 M_c^{Be}(E_c',\theta_c)}{dE_c' d\Omega}, \qquad (A1)$$

where σ_{cf}, σ_C, σ_B and σ_{Be} are, respectively, the cross sections for the complete fusion and the three incomplete fusion processes.

For σ_{cf} we used the value 590 mb given by [14]. For σ_C, σ_{Be} and σ_B we used the values of, respectively 500, 70 and 50 mb. σ_B was estimated by assuming that in most cases, after the projectile's break-up the not observed fragment fuses with the target nucleus (i.e. assuming dominance of break-up-fusion processes) and an almost equal probability of observing, in such a process either fragment, if their mass does not differ considerably. In these hypotheses σ_B is about equal to the angle-integrated cross section for B production in the ^{16}O break-up, which we found to be about 50 mb. The sum of σ_C and σ_{Be} ($\approx$ 570 mb) was then obtained by subtracting from the estimated reaction cross section ($\approx$ 2730 mb) [14] (a) the complete fusion cross section (590 mb), (b) the measured cross section for production of ^{12}C by ^{16}O break-up which we found to be ($\approx$ 180 mb), (c) the double of the measured cross section for production of ^{15}N ($\approx$ 320 mb) (assuming equal cross sections for producing ^{15}N and ^{15}O by, respectively, proton and neutron transfer), (d) the cross section for production of Li and B estimated to be the double of the measured cross section for producing B (about 100 mb) and (e) an estimated inelastic scattering cross section of about 650 mb. The value of this cross section was not obtained from the rather scarce and not systematic measurements of inelastic scattering spectra reported in literature, but from the rather accurate measurement of the cross sections of residues with mass slightly smaller than the target nucleus mass in the interaction of ^{16}O with ^{103}Rh [15], at 250 MeV, about one half of which, according to some recent calculations, we deem to be due to the decay of the target nucleus excited in the ^{16}O inelastic scattering. This gives us an inelastic scattering cross section on ^{103}Rh of about 880 mb. Assuming for this cross section an $A^{2/3}$ dependence we finally get the value given above. We know from a recent experiment that the cross section for production of ^{8}Be in ^{16}O break up is quite small and thus reach the conclusion that the cross section for incomplete fusion of C should be about 500 mb. Fig. 4 gives, at various emission angles, the calculated contributions to the carbon spectra due to the complete fusion of ^{16}O and the incomplete fusion of ^{12}C, ^{8}Be and ^{10}B. Considering that the prediction of the incomplete fusion cross section given by the systematics may be considered quite accurate, one may see that the main source of error comes from the estimate of the cross section for ^{12}C incomplete fusion. Assuming a quite large error of about 30% in the estimate of this cross section, which even considering the many assumptions which we have made we think to be a resonable estimate, this will give an uncertainty of about 10% to the calculated coalescence cross section, a value which we consider to be tolerable in the absence of experimental measurements of all the cross sections of the different processes which may occur in the interaction of ^{16}O with ^{59}Co.

Acknowledgements

We wish to thank M. Pigni for his help in the BME calculations and Prof. A. A. Cowley for useful discussions on drafting this manuscript.

References

1. E. Gadioli, M. Cavinato, E. Fabrici, E. Gadioli Erba, R. Bassini, C. Birattari, S. Crippa, G. F. Steyn, S. V. Förtsch, J. J. Lawrie, F. M. Nortier, S. H. Connell, E. Sideras Haddad, J. P. F. Sellschop and A. A. Cowley, Eur. Phys. J. A **8** (2000) 373.
2. H. Fröhlich, T. Shimoda, M. Ishihara, K. Nagatami, T. Udagawa and T. Tamura, Phys. Rev. Lett. **42** (1979) 1518.
3. T. Udagawa, T.Tamura, T. Shimoda, H. Fröhlich, M. Ishihara and K. Nagatami, Phys. Rev. C**20** (1979) 1949.
4. M. S. Hussein, K. W. Mc Voy and D. Saloner, Phys. Lett. **98B** (1981) 162.
5. T. C. Awes, G. Poggi, C. K. Gelbke, B. B. Back, B. G. Glagola, H. Breuer and V. E. Viola, Phys, Rev. C **24** (1981) 89.
6. T. C. Awes, S. Saini, G. Poggi, C. K. Gelbke, D. Cha, R. Legrain, and G. D. Westfall, Phys. Lett. C**25** (1982) 2361.
7. I. Cervesato, M. Cavinato, E. Fabrici, E. Gadioli, E. Gadioli Erba and M. Galmarini, Phys. Rev. C**45** (1992) 2369.
8. M. Cavinato, E. Fabrici, E. Gadioli, E. Gadioli Erba, M. Galmarini and A. Gritti, Z. Phys. A**347** (1994) 237.
9. M. Cavinato, E. Fabrici, E. Gadioli, E. Gadioli Erba and E. Risi, Nucl. Phys. **A643** (1998) 15.
10. M. Cavinato, E. Fabrici, E. Gadioli, E. Gadioli Erba and G. Riva, Nucl. Phys. **A679** (2001) 753.
11. C. Brusati, M. Cavinato, E. Fabrici, E. Gadioli and E. Gadioli Erba, Z. Phys. **A353** (1995) 57.
12. J. Hill and J. A. Wheeler, Phys. Rev. **89** (1953) 1102.
13. J. Gomez del Campo, Phys. Rev. Lett. **61** (1988) 290.
14. W. W. Wilcke, J. R. Birkelund, H. J. Wollersheim, A. D. Hoover, J. R. Huizenga, W. U. Scröder and L. E. Tubbs, Atomic Data and Nucl. Data Tables. **25** (1980) 389.
15. E. Gadioli, C. Birattari, M. Cavinato, E. Fabrici, E. Gadioli Erba, V. Allori, F. Cerutti, A. Di Filippo, S. Vailati, T. G. Stevens, S. H. Connell, J. P. F. Sellschop, F. M. Nortier, G. F. Steyn, and C. Marchetta, Nucl. Phys. **A641** (1998) 271.